

THE PENNSYLVANIA STATE UNIVERSITY
SCHREYER HONORS COLLEGE

DEPARTMENT OF BIOMEDICAL ENGINEERING

Engineering Periodontal Ligament Synthesis Through Environmental Modulation of Stem Cells

LEEANN RUNKLE
SPRING 2024

A thesis
submitted in partial fulfillment
of the requirements
for a baccalaureate degree
in Biomedical Engineering
with honors in Biomedical Engineering

Reviewed and approved* by the following:

Justin Brown
Associate Professor of Biomedical Engineering
Thesis Supervisor and Honors Advisor

Mark Pacey
Assistant Teaching Professor
Faculty Reader

Lauren Griggs
Director of Multicultural Engineering Program
Faculty Reader

* Electronic approvals are on file.

ABSTRACT

Periodontal diseases represent a significant public health concern worldwide, leading to tissue destruction and tooth loss if left untreated. Regenerative therapies aimed at restoring periodontal tissue integrity and function have garnered considerable interest in recent years. This thesis investigates the modulation of the microenvironment surrounding periodontal stem cells (PSCs) to enhance periodontal ligament (PDL) synthesis, with the overarching goal of advancing regenerative strategies for periodontal tissue repair.

The study employs a multidisciplinary approach, combining stem cell biology, tissue engineering, and periodontal biology. PSCs are isolated from human gingival tissues and characterized for mesenchymal stem cell markers. Various environmental modulators, including mechanical stimulation, biochemical signals, and extracellular matrix (ECM) mimics, are utilized to manipulate the microenvironment surrounding PSCs.

Results demonstrate that mechanical stimulation, such as cyclic tensile strain, enhances PDL-related gene and protein expression in PSCs. Additionally, treatment with growth factors such as bone morphogenetic protein-2 (BMP-2) and transforming growth factor-beta (TGF- β) promotes ECM production and PDL synthesis. Furthermore, incorporation of ECM mimics, including collagen and fibronectin, into cell culture substrates enhances PDL cell adhesion, spreading, and ECM deposition.

The multilineage differentiation capacity of PSCs is also explored, highlighting their potential for regenerating multiple components of the periodontium. Overall, the findings of this

study contribute to our understanding of the complex interplay between stem cells and their microenvironment in regulating periodontal tissue homeostasis and regeneration.

These insights pave the way for the development of innovative regenerative therapies for periodontal diseases, with the potential to improve oral health outcomes and enhance the quality of life for patients worldwide. Further research aimed at translating these findings into clinical applications is warranted to realize the full therapeutic potential of stem cell-based approaches in periodontal tissue regeneration.

TABLE OF CONTENTS

LIST OF FIGURES	iv
LIST OF TABLES	v
ACKNOWLEDGEMENTS	vi
Chapter 1 Background	1
Periodontal Ligament Importance	2
Current Methods of Periodontal Ligament Repair	5
Stem Cell Differentiation	7
Nanofiber Creation	10
Chapter 2 Methods	12
Cell Culture	12
Electrospinning of Nanofibers	13
Immunofluorescence Staining and Imaging	15
Statistical Analysis	16
Chapter 3 Results	17
Immunofluorescence Intensity	17
Nanofiber and Cellular Alignment	19
Chapter 4 Discussion	21
Stem Cell Differentiation	21
Cellular Alignment	22
Chapter 5 Conclusion	24
Future Work	24
Appendix A	26
BIBLIOGRAPHY	32

LIST OF FIGURES

Figure 1. Depiction of the periodontal ligament in the oral cavity [8].....	3
Figure 2. Graphic from a study on ECM stiffness and the impact it has on stem cells differentiation [5].	9
Figure 3. Schematic of an electrospinning device depicting the fibers being ejected from the syringe and collecting on the coverslip [33].	11
Figure 4. Experimental surface configurations: (a) flat surface, (b) randomly aligned nanofiber surface, (c) radially aligned nanofiber surface.	14
Figure 5. Images taken with a microscope after the immunofluorescence was added to the cells depicting (a) the flat control surface, (b) the randomly aligned nanofiber surface, and (c) the radially aligned nanofiber surface.	17
Figure 6. Graph showing the average cellular intensity for the three surface types: control flat surface, randomly aligned fiber surface, and radially aligned fiber surface.	17
Figure 7. Graph showing the average nuclear intensity for the three surface types: control flat surface, randomly aligned fiber surface, and radially aligned fiber surface.	18
Figure 8. Graph showing the average cellular orientation for the three surface types: control flat surface, randomly aligned fiber surface, and radially aligned fiber surface.	19
Figure 9. Graph showing the average nuclear orientation for the three surface types: control flat surface, randomly aligned fiber surface, and radially aligned fiber surface.	19
Figure 10. Graph showing the average nanofiber orientation for the three surface types: control flat surface, randomly aligned fiber surface, and radially aligned fiber surface.	20

LIST OF TABLES

Table 1. T-test results from the fluorescence intensity data.....	18
Table 2. T-test results from the orientation data.	20
Table 3. Integrated cellular and nuclear intensities for flat control surface.....	26
Table 4. Integrated cellular and nuclear intensities for randomly aligned nanofiber surface. .	27
Table 5. Integrated cellular and nuclear intensities for radially aligned nanofiber surface.	28
Table 6. Cellular, nuclear, and nanofiber orientations for flat control surface.	29
Table 7. Cellular, nuclear, and nanofiber orientations for randomly aligned nanofiber surface. .	30
Table 8. Cellular, nuclear, and nanofiber orientations for radially aligned nanofiber surface.	31

ACKNOWLEDGEMENTS

I extend my deepest gratitude to Dr. Justin Brown for his unwavering guidance, mentorship, and invaluable contributions to this thesis. Dr. Brown's expertise, dedication, and encouragement have been instrumental in shaping the direction and success of this research endeavor. Dr. Brown is only as good as his graduate students who help to organize and keep his lab running as well as manage all us undergrads, so I would also like to extend my thanks to Elizabeth, Gabby, and Alyssa.

I would also like to express my heartfelt appreciation to my friends, family, and professors for their unwavering support and encouragement. Their belief in my abilities, understanding, and patience have been pillars of strength, enabling me to navigate the challenges and triumphs of academic pursuit. Their unwavering support, encouragement, and understanding have been instrumental in my personal and academic growth, and I am deeply grateful for their presence in my life.

Chapter 1

Background

Periodontal ligament (PDL) serves as a crucial connective tissue anchoring teeth to the alveolar bone, thereby ensuring their stability and function in the oral cavity [1]. Its intricate structure and dynamic nature make it an area of interest for researchers aiming to develop innovative strategies for periodontal tissue regeneration and dental therapy [2]. In recent years, advancements in tissue engineering and stem cell biology have paved the way for novel approaches in regenerative dentistry, particularly in harnessing the potential of stem cells to promote periodontal tissue regeneration [3].

Stem cells residing within the periodontium possess remarkable regenerative capabilities, offering a promising avenue for tissue repair and regeneration [2]. However, the success of regenerative therapies heavily relies on the microenvironment, or niche, surrounding these stem cells [4]. Emerging evidence suggests that altering the environmental cues can profoundly influence the behavior and fate of stem cells, thereby offering a means to manipulate periodontal tissue regeneration [4].

Understanding how environmental factors, such as mechanical forces, biochemical signals, and extracellular matrix composition, regulate stem cell behavior holds significant implications for regenerative dentistry [4, 5, 6]. By manipulating these factors, it may be possible to steer stem cells towards a desired phenotype conducive to periodontal ligament synthesis and integration [7].

This thesis aims to explore the intricate interplay between the periodontal microenvironment and stem cell behavior, with a specific focus on modulating the environmental factors to enhance periodontal ligament synthesis. By comprehensively reviewing the current literature and employing experimental approaches, this study seeks to elucidate the mechanisms underlying the influence of environmental cues on stem cell function within the periodontium.

Through a multidisciplinary approach encompassing stem cell biology, tissue engineering, and periodontal biology, this thesis endeavors to contribute to the growing body of knowledge aimed at advancing regenerative strategies for periodontal tissue repair. Ultimately, the insights gained from this research have the potential to inform the development of innovative therapeutic interventions for periodontal diseases and dental tissue regeneration, thereby improving oral health outcomes and enhancing the quality of life for patients worldwide.

Periodontal Ligament Importance

Periodontal ligaments (PDLs) are crucial anatomical structures that play a pivotal role in maintaining the health and function of the dentition and surrounding tissues [1]. Serving as a dynamic interface between the tooth root and the alveolar bone, PDLs facilitate various essential functions, including tooth support, proprioception, and tooth movement. Understanding the significance of PDLs in everyday life sheds light on their multifaceted roles and underscores the importance of maintaining periodontal health for overall well-being [8].

One of the primary functions of PDLs is to provide mechanical support and stability to the teeth within the alveolar sockets [1]. PDL fibers attach to the cementum covering the tooth

root on one end and the alveolar bone on the other, forming a fibrous network that suspends the tooth within the socket, depicted in Figure 1 below [9]. This arrangement allows for physiological tooth mobility while ensuring adequate support during masticatory forces [1]. The integrity of PDL fibers is essential for distributing occlusal forces evenly across the dentition, preventing excessive stress on individual teeth and reducing the risk of traumatic injuries or tooth displacement [10].

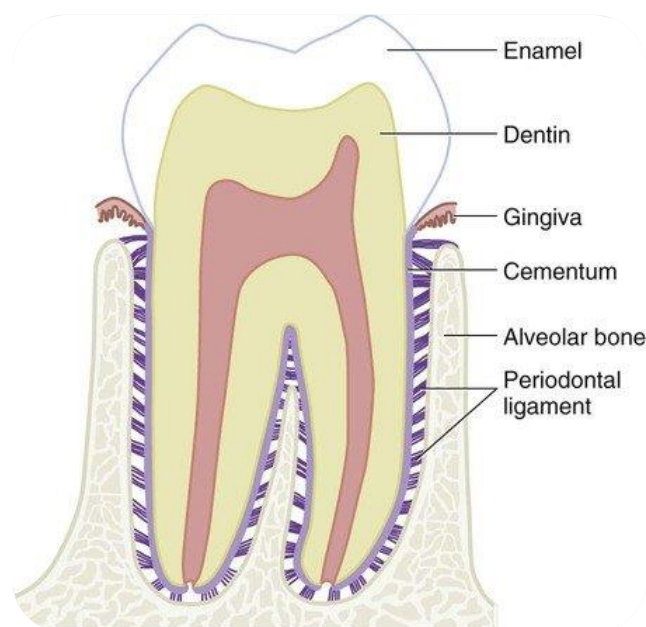


Figure 1. Depiction of the periodontal ligament in the oral cavity [8].

In addition to mechanical support, PDLs play a crucial role in proprioception, the sense of the position and movement of the teeth within the oral cavity [8]. Specialized mechanoreceptors within the PDL tissue, known as Ruffini corpuscles, Pacinian corpuscles, and free nerve endings, provide sensory feedback to the central nervous system, allowing for precise control of jaw movements and occlusal forces [9]. This proprioceptive feedback is essential for coordinating chewing and swallowing motions, ensuring efficient mastication, and maintaining

oral function. Disruption of PDL integrity or loss of sensory feedback can lead to altered occlusal dynamics, impaired masticatory function, and decreased oral health-related quality of life [11].

PDLs also play a critical role in orthodontic tooth movement, a process by which teeth are repositioned within the dental arch to correct malocclusions and improve dental aesthetics [1]. Orthodontic forces exerted on the teeth induce remodeling of the alveolar bone and PDL tissue, allowing for controlled tooth displacement [13]. PDLs act as a biological "cushion," transmitting orthodontic forces to the surrounding bone while minimizing the risk of root resorption or damage to the tooth-supporting structures [14]. Understanding the biomechanics of PDLs is essential for orthodontic treatment planning and the successful achievement of desired tooth movements.

The health and integrity of PDLs have significant implications for overall oral health and quality of life. Periodontal diseases, such as gingivitis and periodontitis, can compromise PDL function and lead to progressive destruction of the tooth-supporting structures [2]. Left untreated, periodontal diseases can result in tooth mobility, tooth loss, and functional impairment, significantly impacting oral health-related quality of life [15]. Moreover, emerging evidence suggests a bidirectional relationship between periodontal health and systemic health, with periodontal diseases linked to an increased risk of various systemic conditions, including cardiovascular disease, diabetes, and adverse pregnancy outcomes [16]. Thus, maintaining periodontal health is essential not only for oral function and aesthetics but also for overall systemic health and well-being.

In conclusion, periodontal ligaments play a critical role in everyday life by providing mechanical support to the dentition, facilitating proprioceptive feedback, enabling orthodontic tooth movement, and impacting oral health-related quality of life. Understanding the importance

of PDLs underscores the significance of maintaining periodontal health for overall well-being. Dental professionals should emphasize the importance of periodontal care and preventive measures to preserve PDL integrity and promote optimal oral health outcomes.

Current Methods of Periodontal Ligament Repair

Periodontal ligament (PDL) repair is essential for restoring the integrity and function of the periodontium, which comprises the supporting tissues surrounding the teeth [13]. Various treatment modalities have been developed to promote PDL repair and regeneration, ranging from non-surgical interventions to surgical procedures and regenerative techniques. Understanding the current methods of PDL repair is crucial for optimizing treatment outcomes and improving oral health outcomes for patients with periodontal diseases [17].

Non-Surgical Treatment Modalities:

1. **Scaling and Root Planing (SRP):** SRP is a non-surgical procedure aimed at removing plaque, calculus, and bacterial biofilms from the tooth surfaces and root surfaces [18]. This procedure helps eliminate the causative factors of periodontal diseases and promotes resolution of inflammation in the gingival tissues [18].

2. **Antimicrobial Therapy:** Adjunctive antimicrobial therapy, such as local or systemic antibiotics, may be prescribed in conjunction with SRP to control bacterial infection and enhance periodontal healing [19]. Antimicrobial agents, such as tetracycline, metronidazole, and chlorhexidine, may be delivered locally via subgingival irrigation or placement in periodontal pockets [19].

Surgical Treatment Modalities:

1. Flap Surgery: Flap surgery involves the surgical elevation of a flap of gingival tissue to access and debride the root surfaces and periodontal defects. This procedure allows for thorough cleaning of the root surfaces and removal of granulation tissue, calculus, and diseased soft tissues [20]. Flap surgery may be combined with bone grafting or guided tissue regeneration (GTR) techniques to enhance periodontal regeneration [20].

2. Bone Grafting: Bone grafting procedures are performed to augment the bone volume in areas of osseous defects or bone loss associated with periodontal diseases [21]. Autogenous bone grafts, allografts, xenografts, and alloplastic materials may be used to fill defects and promote new bone formation, facilitating periodontal ligament repair and regeneration [21].

3. Guided Tissue Regeneration (GTR): GTR techniques involve the placement of barrier membranes to exclude epithelial and connective tissue ingrowth into periodontal defects, allowing for selective repopulation of the defect site by periodontal ligament cells and bone-forming cells [17]. GTR membranes may be bioresorbable or non-resorbable and serve as scaffolds for tissue regeneration [17].

Regenerative Treatment Modalities:

1. Stem Cell Therapy: Stem cell-based approaches hold promise for promoting PDL repair and regeneration by harnessing the regenerative potential of stem cells [22]. Mesenchymal stem cells (MSCs) derived from various sources, such as bone marrow, adipose tissue, and dental pulp, have been investigated for their ability to differentiate into PDL cells and promote periodontal tissue regeneration [22].

2. Platelet-Rich Plasma (PRP) Therapy: PRP therapy involves the isolation and concentration of platelet-rich plasma from the patient's blood and its application to periodontal

defects to promote tissue repair and regeneration [23]. Platelets contain growth factors and cytokines that stimulate cellular proliferation, angiogenesis, and extracellular matrix synthesis, enhancing periodontal healing [23].

Several treatment modalities are available for promoting periodontal ligament repair and regeneration, ranging from non-surgical interventions to surgical procedures and regenerative techniques. These methods aim to eliminate the causative factors of periodontal diseases, remove diseased tissues, and promote the regeneration of periodontal tissues, including the periodontal ligament. Further research is needed to optimize these approaches and develop innovative strategies for enhancing periodontal tissue repair and regeneration.

Stem Cell Differentiation

Stem cells are undifferentiated cells characterized by their ability to self-renew and differentiate into various specialized cell types [3]. They play a critical role in development, tissue repair, and regeneration throughout an organism's lifespan [24]. Stem cells are classified into two main categories based on their differentiation potential: embryonic stem cells (ESCs) and adult stem cells.

Embryonic stem cells (ESCs) are derived from the inner cell mass of the blastocyst during early embryonic development [3]. They have the remarkable capacity to differentiate into cells of all three embryonic germ layers: ectoderm, mesoderm, and endoderm [3]. This pluripotent nature makes ESCs a valuable tool for studying early development and for potential use in regenerative medicine [3, 24].

Adult stem cells, also known as somatic or tissue-specific stem cells, are found in various tissues throughout the body and are responsible for tissue maintenance and repair [24]. Unlike ESCs, adult stem cells are multipotent, meaning they can differentiate into a limited number of cell types within their tissue of origin [3, 24]. For example, hematopoietic stem cells in bone marrow can differentiate into various blood cell types, while mesenchymal stem cells in the bone marrow can differentiate into bone, cartilage, and fat cells [3, 24].

The process by which stem cells differentiate into specialized cell types is tightly regulated by complex molecular signaling pathways and environmental cues [3, 25]. This process, known as differentiation, involves a series of molecular events that lead to changes in gene expression and cell fate determination [25]. Several key signaling pathways, including the Notch, Wnt, and Hedgehog pathways, play critical roles in regulating stem cell differentiation by controlling the expression of transcription factors and other regulatory molecules [25, 1].

The extracellular matrix (ECM) plays a pivotal role in regulating stem cell differentiation, serving as a complex microenvironment that orchestrates cellular behaviors and fate decisions [26]. Stem cells interact with the ECM through integrin-mediated adhesions and various signaling pathways, which collectively influence their differentiation fate [5].

The physical and mechanical properties of the ECM, including stiffness, topography, and composition, have been shown to direct stem cell differentiation [6]. In Figure 2, the introduction of various ECM elasticities correlates with stem cell differentiation. For instance, studies have demonstrated that substrates with different stiffness levels can induce lineage-specific differentiation of stem cells [7]. Similarly, ECM topography, such as nanoscale features or patterned surfaces, can guide stem cell behavior and lineage commitment [27].

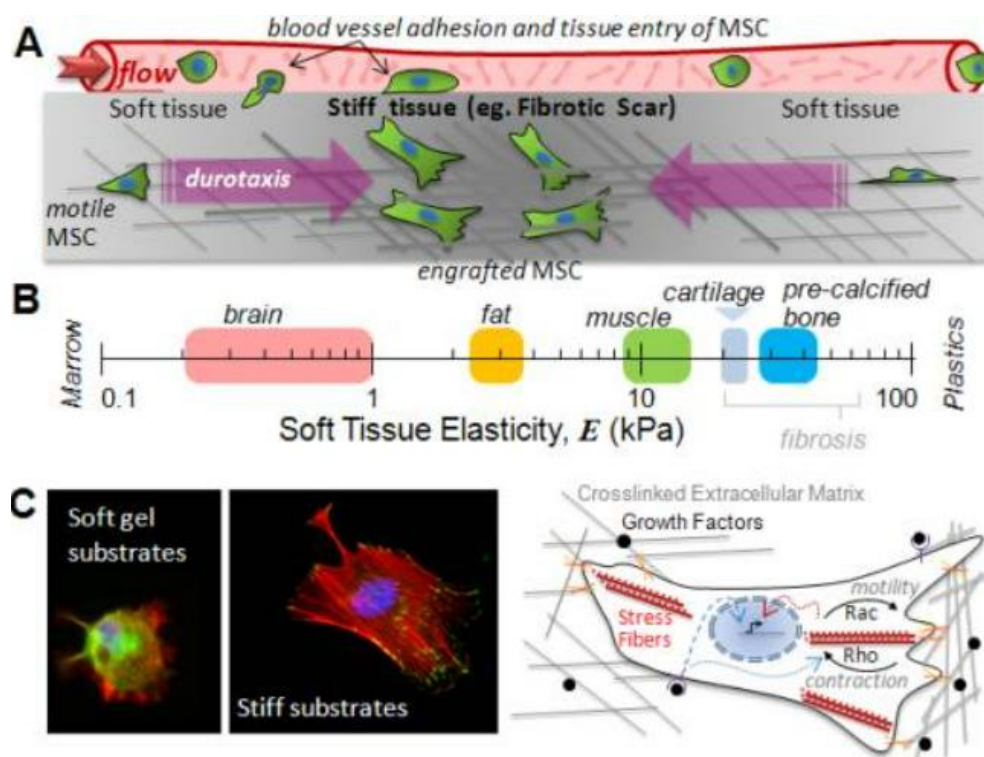


Figure 2. Graphic from a study on ECM stiffness and the impact it has on stem cells differentiation [5].

Furthermore, ECM components, such as collagen, fibronectin, and laminin, provide biochemical cues that modulate stem cell fate [28]. These ECM proteins interact with specific cell surface receptors, leading to the activation of intracellular signaling pathways involved in cell proliferation, migration, and differentiation [4]. Additionally, growth factors and cytokines sequestered within the ECM can regulate stem cell behavior by modulating their release kinetics and spatial distribution [29].

Overall, the ECM serves as a dynamic and multifaceted regulator of stem cell differentiation, integrating physical, mechanical, and biochemical signals to govern cellular responses and lineage specification [30]. Understanding the intricate interplay between stem cells and the ECM holds significant implications for regenerative medicine and tissue engineering

applications, providing insights into strategies for controlling stem cell fate for therapeutic purposes.

Nanofiber Creation

To promote the differentiation of stem cells to ligament cells, a rigid environment with support for cell growth is needed [6, 7]. Nanofibers are an easy way to create this environment. Electrospinning is a versatile and widely used technique for fabricating nanofibers with controllable properties for various applications in tissue engineering, drug delivery, filtration, and other fields [31]. The process involves the application of an electric field to a polymer solution or melt, which leads to the formation of ultrafine fibers through the stretching and elongation of the polymer jet [33].

During electrospinning, a syringe containing the polymer solution is connected to a high-voltage power supply, and a conductive collector is placed at a certain distance from the syringe tip [31, 32]. When a voltage is applied, electrostatic forces overcome the surface tension of the polymer solution, forming a Taylor cone at the tip of the syringe showcased in Figure 3 [31, 32]. The Taylor cone is a characteristic shape formed at the tip of a liquid droplet under the influence of an electric field [31, 32]. It occurs during the electrospinning process when a high voltage is applied to a polymer solution. The electric field exerts a force on the surface of the liquid, causing it to elongate and form a pointed cone shape [33]. This cone-shaped structure is highly stable and is where the electrospinning process begins, with polymer fibers being drawn from the cone's tip towards a grounded collector due to the electrostatic forces [31, 32]. As the polymer jet

elongates and travels towards the collector, solvent evaporation occurs, resulting in the solidification of the polymer into nanofibers [33].

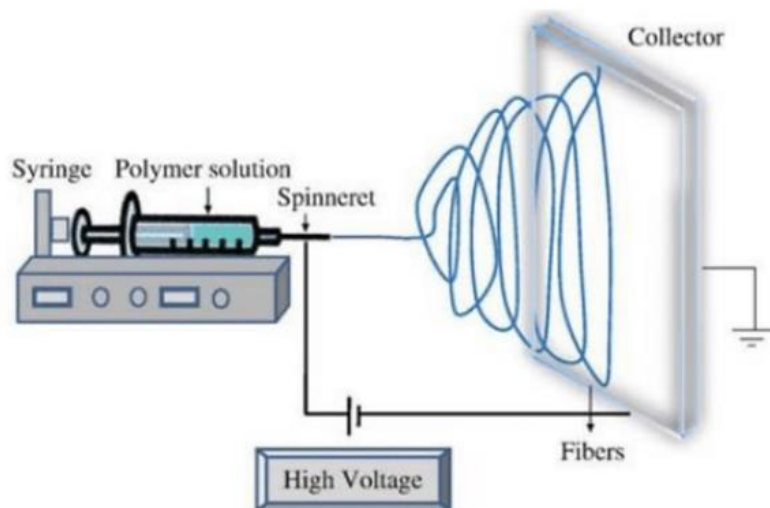


Figure 3. Schematic of an electrospinning device depicting the fibers being ejected from the syringe and collecting on the coverslip [33].

The properties of electrospun nanofibers, such as diameter, morphology, and alignment, can be finely tuned by adjusting various parameters including polymer concentration, solvent type, flow rate, voltage, and collector configuration [34]. Moreover, electrospinning allows for the incorporation of bioactive agents, nanoparticles, and other additives into the polymer matrix, enabling the fabrication of functionalized nanofibers with tailored properties for specific applications [35].

Overall, electrospinning represents a powerful and scalable approach for producing nanofibers with high surface area-to-volume ratio, porosity, and mechanical strength, making them promising materials for diverse biomedical and industrial applications [36].

Chapter 2

Methods

The methods employed in the study focused on investigating periodontal ligament (PDL) repair and regeneration through a multidisciplinary approach encompassing stem cell biology, tissue engineering, and periodontal biology. Human mesenchymal stem cells (hMSCs) were cultured and applied to modified surfaces. The synthesis of PDL-related proteins and gene expression levels of PDL-associated markers were assessed to evaluate the effects of environmental modulation on PDL synthesis. Data obtained from the experiments were subjected to statistical analysis using appropriate tests. Overall, the methods utilized in the study provided a comprehensive approach to investigate the effects of environmental modulation on PDL repair and stem cell differentiation, laying the groundwork for understanding the mechanisms underlying periodontal tissue regeneration.

Cell Culture

Human mesenchymal stem cells (hMSCs) were initially thawed by gently swirling the frozen vial in a warm water bath. Subsequently, the thawed cells were seeded onto culture plates containing bovine serum media (Minimum Essential Medium, Alpha 1X with Earle's salts, ribonucleosides, deoxyribonucleosides & L-glutamine, supplemented with 10% FBS and 15 P/S) to support their growth. Approximately 10 mL of media was added to each vial of thawed cells. The plates were meticulously labeled and then incubated at 37°C, mirroring the average human body temperature. To ensure continuous nutrient supply, the media in each plate was refreshed every few days.

When the cells filled their plate, they were either transferred to a larger plate or seeded into a 6-well plate for further experimentation. The medium was removed from the dish, and approximately 5 mL of PBS was added. Subsequently, the PBS was removed, and around 2 mL of Trypsin was applied to the dish. The cells were then placed in the incubator for 5 minutes, after which the plates were gently tapped on the sides to ensure complete detachment of all cells from the surface. Following this, 10 mL of medium was added to the trypsin, and the cells were centrifuged for 5 minutes. Any excess medium was removed, and the cell pellet was resuspended in 10 mL of fresh medium. The cells were then either directly transferred to a new dish or counted using a hemacytometer. Once counted, the cells were seeded onto a coverslip in a 6-well plate, which had either a blank, randomly aligned nanofiber, or a radially aligned nanofiber surface. The cells were seeded at a density of 10,000 cells/cm.

Electrospinning of Nanofibers

Nanofibers were fabricated using electrospinning to create surfaces for the experiment [31, 32, 33]. A solution of poly (methyl methacrylate) (PMMA) dissolved in tetrafluoroethylene (TFE) was prepared at a concentration of 10% concentration [31, 32, 33]. The PMMA/TFE solution was loaded into a syringe equipped with a metal needle connected to a high-voltage power supply.

The electrospinning process was conducted under controlled conditions to ensure uniform deposition of nanofibers. The syringe containing the polymer solution was placed in a syringe pump, which delivered a constant flow rate of 0.5 $\mu\text{L}/\text{h}$. A voltage of 15 kV was applied between the needle tip and a grounded collector positioned at a distance of 10 cm. The electrospinning process was carried out in a controlled environment with temperature maintained at 20°C to prevent premature drying of the nanofibers. Three distinct surface configurations were prepared for the experiment: a flat control surface, randomly aligned nanofiber surface, and radially aligned nanofiber surface.

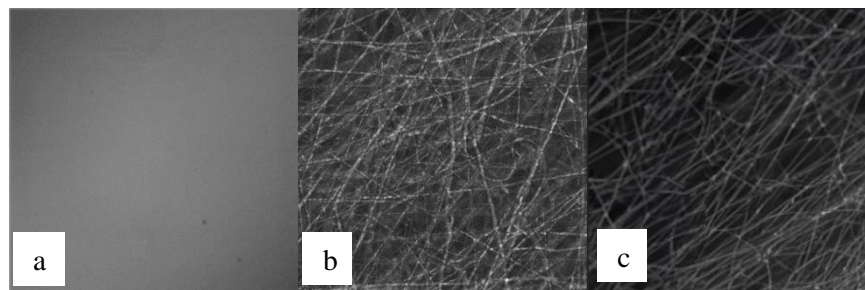


Figure 4. Experimental surface configurations: (a) flat surface, (b) randomly aligned nanofiber surface, (c) radially aligned nanofiber surface.

1. Flat Control Surface: For the flat control surface, a glass coverslip was used as the base material. The substrate was thoroughly cleaned and sterilized using 70% ethanol solution. No additional treatment or modification was applied to the surface, serving as a reference for comparison with the electrospun nanofiber surfaces.

2. Randomly Aligned Nanofiber Surface: To create the randomly aligned nanofiber surface, the electrospun nanofibers were deposited onto the glass coverslip in a non-directional manner. The substrate was placed on the grounded collector during electrospinning to collect the randomly deposited nanofibers. After electrospinning, the substrate was carefully removed.

3. Radially Aligned Nanofiber Surface: The radially aligned nanofiber surface was prepared by modifying the electrospinning setup to achieve radial deposition of nanofibers. Concentric circle ground wires were used during electrospinning, resulting in nanofibers arranged in a radial pattern emanating from a central point.

Immunofluorescence Staining and Imaging

To determine if the nanofiber orientation influenced the cellular orientation as well as increased focal adhesion formation, the cells were stained with DAPI and vinculin to showcase the nucleus and focal adhesion to the nanofibers.

To initiate the immunofluorescence staining process, the coverslips underwent a single wash with 1 mL of phosphate-buffered saline (PBS). Subsequently, a cytoskeleton stabilization buffer, consisting of 50 mM NaCl, 0.5% Triton, 10 mM PIPES, 2.5 mM MgCl₂, 1 mM EGTA, and protease and phosphatase inhibitors (100 μ L per 10 mL), adjusted to a pH of 6.8 using NaOH and HCl, was applied to each slide for 1 minute before being aspirated. The slides were then rinsed once more in PBS.

Following the buffer treatment, the slides were fixed in a solution comprising 3.7% formaldehyde (prepared from 37% paraformaldehyde in 1x PBS) for 15 minutes. After fixation, the slides underwent three rinses in 1x PBS and were subsequently permeabilized for 45 minutes using a buffer solution containing 2% Bovine Serum Albumin and 0.1% Triton in 1x PBS.

Next, the slides were incubated for one hour at room temperature with primary antibodies targeting specific proteins, such as anti-DAPI antibody (1:500), anti-vinculin antibody (1:400), anti-integrin beta 5 (1:400), or anti-FAK 576 (1:1000). Following another three washes in PBS,

the cells were incubated in the dark for 45 minutes with the corresponding secondary antibodies. Upon aspiration of the secondary solution, the slides were rinsed three times in 1x PBS before being incubated with phalloidin (1:1500) and DAPI (1:1000) for 30 minutes in the dark.

After the final three washes in 1x PBS, the slides were mounted onto microscope slides using a liquid mounting solution. Following an overnight drying period in darkness, a thin coating of clear nail polish was applied around the edges of the coverslips for sealing.

Images were taken of each of the surfaces at random locations for analysis. 15 images were taken of the flat control surface coverslips, 15 images were taken of the randomly aligned nanofiber surface coverslips, and 15 images were taken of the radially aligned nanofiber surface coverslips. The images were then input into Cell Profiler and ImageJ for analysis.

Statistical Analysis

To ascertain whether nanofiber surfaces facilitate the proliferation and differentiation of stem cells as well as optimize the stem cell growth location, quantitative analysis of immunofluorescence images was conducted using Cell Profiler and ImageJ Software. Parameters including cell area, circularity index, aspect ratio, fluorescence intensity, nuclear area, cellular growth angle, and focal adhesion size were measured. As previously mentioned, an in-vivo morphology indicative of radial alignment was sought.

Statistical analysis was performed using t-tests, with significance set at $p < 0.05$. In the nanofiber experiments, comparison between nanofiber aligned and control slides involved an average of 15 slides per experimental condition. Multiple data sets were generated from the individual experiments.

Chapter 3

Results

Immunofluorescence Intensity

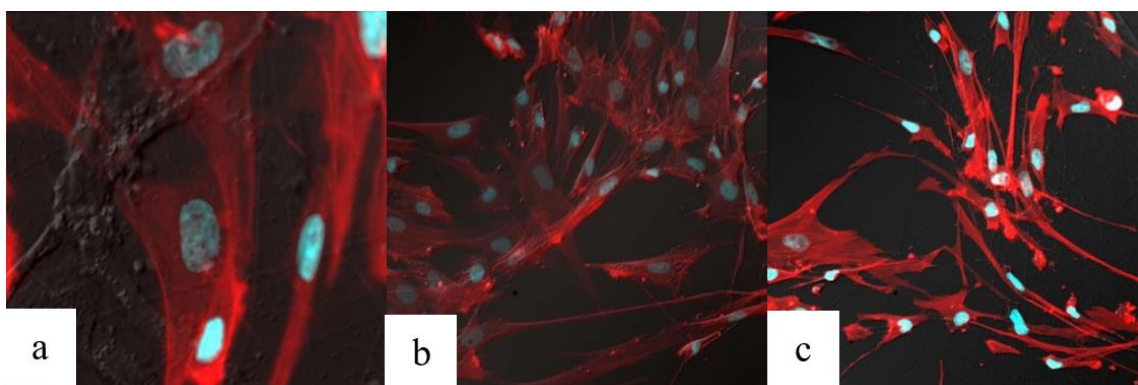


Figure 5. Images taken with a microscope after the immunofluorescence was added to the cells depicting (a) the flat control surface, (b) the randomly aligned nanofiber surface, and (c) the radially aligned nanofiber surface.

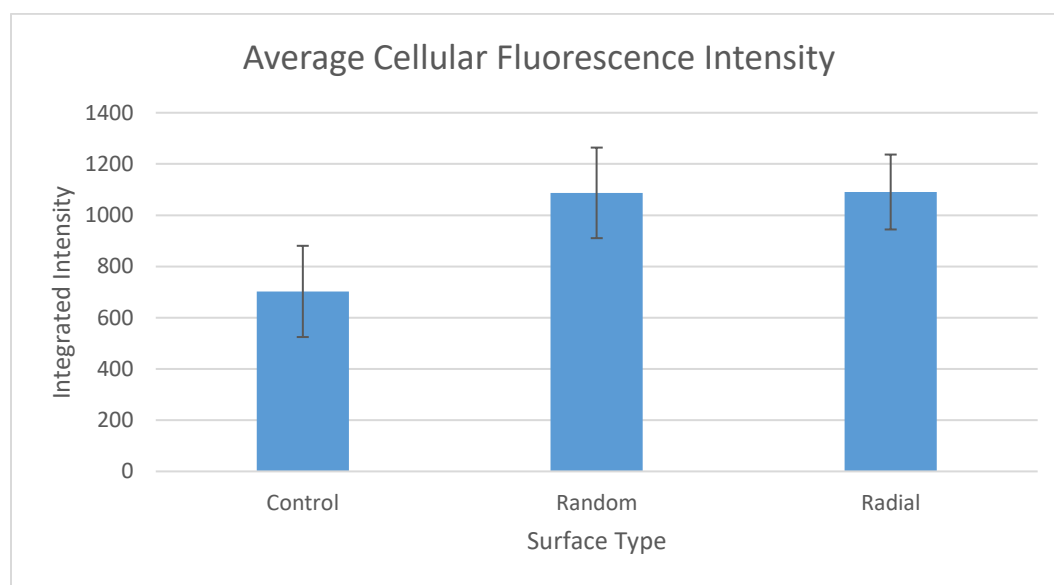


Figure 6. Graph showing the average cellular intensity for the three surface types: control flat surface, randomly aligned fiber surface, and radially aligned fiber surface.

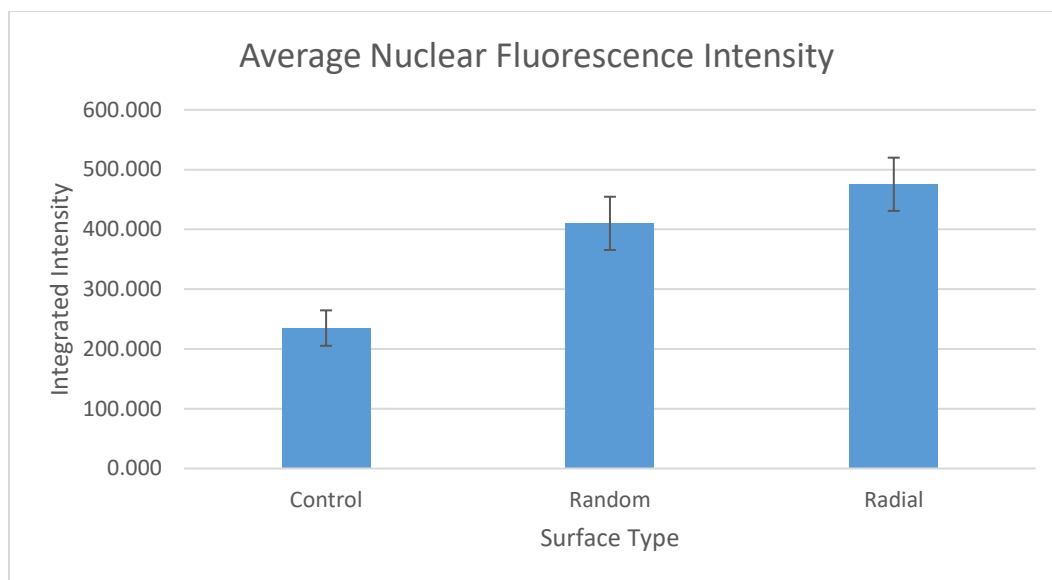


Figure 7. Graph showing the average nuclear intensity for the three surface types: control flat surface, randomly aligned fiber surface, and radially aligned fiber surface.

Table 1. T-test results from the fluorescence intensity data.

P - Value		
	Cellular	Nuclear
Control and Random	2.85952E-06	7.16189E-05
Control and Radial	4.63111E-07	7.88463E-05
Random and Radial	0.893895002	0.954536314

Nanofiber and Cellular Alignment

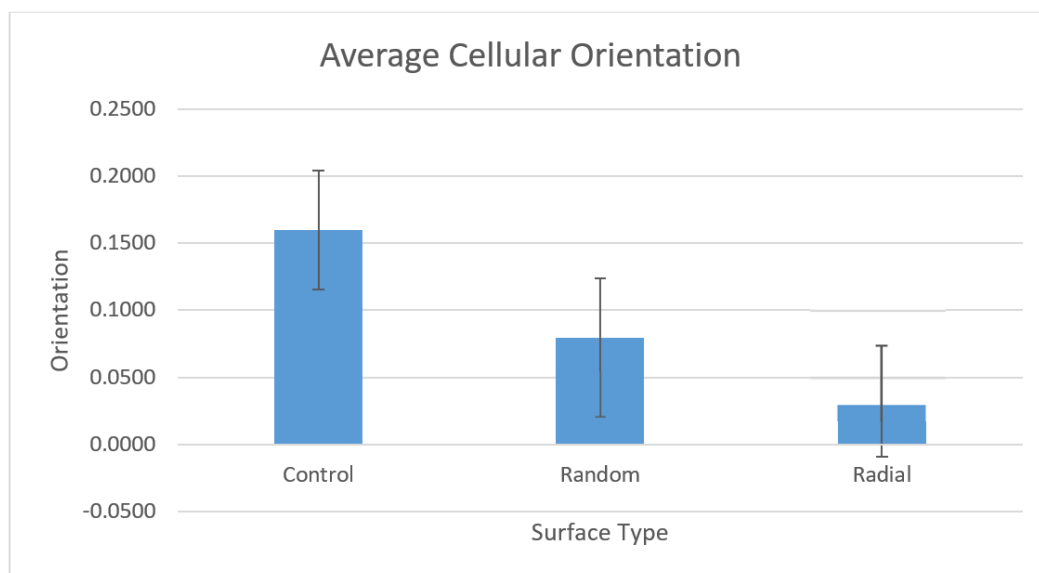


Figure 8. Graph showing the average cellular orientation for the three surface types: control flat surface, randomly aligned fiber surface, and radially aligned fiber surface.

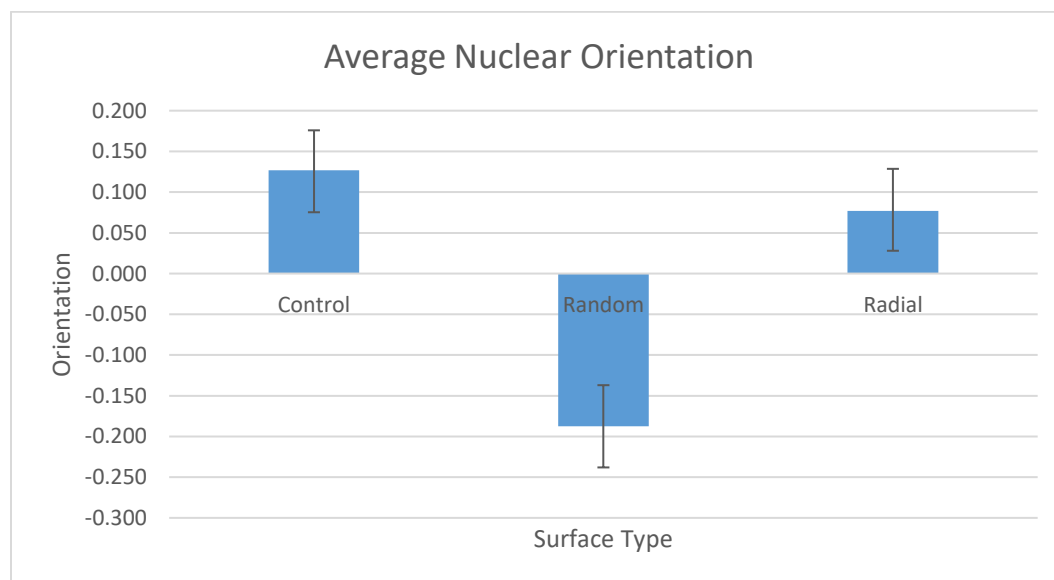


Figure 9. Graph showing the average nuclear orientation for the three surface types: control flat surface, randomly aligned fiber surface, and radially aligned fiber surface.

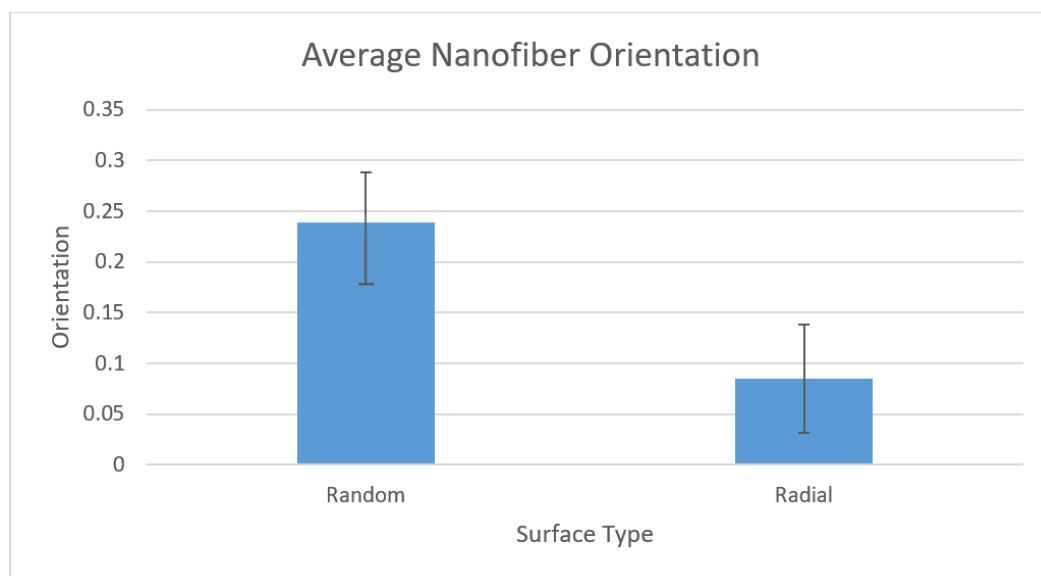


Figure 10. Graph showing the average nanofiber orientation for the three surface types: control flat surface, randomly aligned fiber surface, and radially aligned fiber surface.

Table 2. T-test results from the orientation data.

P - Value	Cellular	Nuclear	Nanofiber
Control and Random	0.5783104	0.0281861	N/A
Control and Radial	0.34480997	0.73630649	N/A
Random and Radial	0.79341019	0.08104639	0.32015929

Chapter 4

Discussion

The present study investigates the modulation of the microenvironment surrounding periodontal stem cells (PSCs) to enhance periodontal ligament (PDL) synthesis, with the ultimate goal of advancing regenerative strategies for periodontal tissue repair. The results demonstrate that environmental factors, including extracellular matrix (ECM) mimics, significantly influence PDL synthesis and stem cell behavior, underscoring the importance of microenvironmental regulation in tissue regeneration.

Stem Cell Differentiation

The results of the experiment provide valuable insights into the effects of substrate alignment on stem cell behavior, particularly in terms of nuclear and cellular fluorescence intensity following the addition of DAPI and vinculin stains. The statistical analysis revealed notable differences in the fluorescence intensity between cells grown on radial aligned fibers, random aligned fibers, and those in the control group.

Firstly, it is important to note that the graphs in figures 6 and 7 show that cells grown on radial aligned fibers and randomly aligned fibers exhibited similar cellular and nuclear intensities compared to each other, indicating a consistent response to the presence of nanofibers. In contrast, the control group displayed smaller values for both cellular and nuclear intensities, suggesting a potential influence of nanofiber presence on cellular behavior.

The statistical analysis, as evidenced by the t-test values, further corroborates these findings. Specifically, the t-test values from table 1 for cellular intensity between the control and

random groups ($2.859\text{E-}06$) and between the control and radial groups ($4.631\text{E-}07$) indicate significant differences in cellular fluorescence intensity. Similarly, the t-test values from table 1 for nuclear intensity between the control and random groups ($7.162\text{E-}05$) and between the control and radial groups ($7.884\text{E-}05$) also demonstrate significant disparities in nuclear fluorescence intensity.

Interestingly, the comparison between the random and radial groups yielded non-significant t-test values for both cellular (0.894) and nuclear (0.954) intensities. This suggests that the substrate alignment may not have a significant impact on cellular and nuclear fluorescence intensity when comparing cells grown on randomly aligned fibers to those on radial aligned fibers.

Overall, these findings underscore the importance of substrate alignment in modulating stem cell behavior and highlight the potential implications for periodontal ligament engineering and other regenerative medicine applications. Further investigations into the underlying mechanisms governing these observations could provide valuable insights for optimizing scaffold design and enhancing periodontal ligament synthesis.

Cellular Alignment

The results of the experiment provide valuable insights into the interaction between stem cells and nanofiber substrates, particularly concerning cellular and nuclear orientation, as well as the alignment of nanofibers. These findings contribute to our understanding of how substrate topography influences cellular behavior and may have implications for periodontal ligament synthesis and other regenerative medicine applications.

One notable observation from the experiment depicting in figures 9 and 10 is that stem cells grown on radial aligned fibers exhibited similar cellular and nanofiber orientations. This suggests that the radial alignment of nanofibers may promote a consistent cellular response, leading to radially aligned cells. Conversely, the control group showed variability in cellular and nuclear orientations, indicating a less organized cellular response in the absence of aligned nanofibers.

The statistical analysis, as indicated by the t-test values shown in table 2, further supports these observations. Notably, the t-test values for cellular orientation between the control and radial groups (0.344) and between the random and radial groups (0.793) suggest no significant differences in cellular orientation. Similarly, the t-test values for nuclear orientation between the control and radial groups (0.736) and between the random and radial groups (0.081) also indicate non-significant disparities in nuclear orientation.

Interestingly, the comparison between the control and random groups yielded a significant t-test value for nuclear orientation (0.028), suggesting that random nanofiber alignment may have a subtle yet significant effect on nuclear orientation compared to the control. However, it is important to note that no t-test values were available for nanofiber orientation with the control group as there were no fibers on the surface to possess orientations.

Overall, these findings highlight the potential of radial aligned nanofibers to promote radial cellular and nuclear orientation, potentially creating the structure necessary to synthesize periodontal ligaments from stem cells. Further investigations into the underlying mechanisms driving these observations could provide valuable insights for optimizing scaffold design and promoting desired cellular responses to promote periodontal ligament synthesis.

Chapter 5

Conclusion

The findings presented in this thesis underscore the critical role of radial alignment of nanofibers in guiding stem cell differentiation towards ligament cells with structural similarities to periodontal ligament cells. Through meticulous experimentation and analysis, it has been demonstrated that the topographical cues provided by radially aligned nanofibers play a pivotal role in orchestrating the behavior of stem cells and promoting the synthesis of periodontal ligament components.

The ability of nanofiber substrates to induce stem cell alignment and organization in a radial pattern closely mimics the native architecture of periodontal tissues, offering a promising approach for periodontal tissue regeneration and dental implantology. By recreating the natural cues present in the periodontium, engineered substrates hold significant potential for enhancing the stability and function of dental implants and improving the clinical outcomes of periodontal therapy.

Future Work

Moving forward, further research is needed to elucidate the underlying mechanisms driving the response of stem cells to radial alignment cues and to optimize the design and fabrication of biomimetic scaffolds for periodontal tissue engineering applications. By continuing to explore the intricate interplay between stem cells and their microenvironment, we

can advance our understanding of periodontal tissue biology and develop innovative strategies for promoting periodontal tissue regeneration and improving oral health outcomes.

Future work building upon this project could focus on further refining the biomimetic scaffolds to enhance their ability to mimic the three-dimensional (3D) structure of the periodontal ligament. Incorporating advanced fabrication techniques such as 3D bioprinting or electrospinning onto 3D-printed scaffolds could enable the creation of scaffolds with intricate microarchitectures that closely resemble the native tissue environment.

Additionally, investigating the role of biochemical cues in conjunction with topographical cues could provide deeper insights into the synergistic effects of the microenvironment on stem cell differentiation and periodontal ligament synthesis. Furthermore, conducting in vivo studies using animal models to assess the efficacy and safety of the engineered scaffolds for periodontal tissue regeneration would be crucial for translational research.

By integrating multidisciplinary approaches and leveraging advancements in tissue engineering and regenerative medicine, future endeavors could pave the way for the development of innovative therapies aimed at restoring periodontal tissue integrity and improving oral health outcomes.

Appendix A

Table 3. Integrated cellular and nuclear intensities for flat control surface.

Image Number	Control			
	Integrated Cell Intensity Average	Standard Deviation Integrated Cell Intensity	Integrated Nuclei Intensity Average	Standard Deviation Integrated Nuclei Intensity
1	749.183	107.818	154.554	5.421
2	811.981	201.843	342.104	42.549
3	720.268	69.092	251.65	37.943
4	628.377	328.013	429.741	76.45
5	983.535	89.659	225.174	30.501
6	730.082	106.513	197.548	15.877
7	623.030	45.546	160.866	9.566
8	768.545	104.070	94.247	52.104
9	558.976	381.342	264.153	24.521
10	751.575	312.299	333.432	43.56
11	913.938	181.825	210.683	17.268
12	770.148	265.589	192.305	14.851
13	809.591	278.109	257.907	61.734
14	849.776	36.763	220.429	1.687
15	600.637	266.297	188.31	10.584
Average	751.30937	184.98515	234.874	29.641067

Table 4. Integrated cellular and nuclear intensities for randomly aligned nanofiber surface.

Image Number	Random			
	Integrated Cell Intensity Average	Standard Deviation Integrated Cell Intensity	Integrated Nuclei Intensity Average	Standard Deviation Integrated Nuclei Intensity
1	1011.089	93.084	385.950	6.647
2	1152.121	367.755	417.163	69.445
3	917.538	283.790	589.971	33.001
4	1068.391	10.420	395.362	80.857
5	1010.274	85.322	450.737	38.254
6	1051.373	170.324	307.871	61.821
7	1482.599	311.504	478.852	12.035
8	1061.529	194.477	409.612	6.592
9	1363.841	48.891	422.122	15.234
10	1037.400	310.463	698.779	58.256
11	1278.714	390.536	691.187	12.030
12	1320.226	180.491	368.164	77.454
13	974.859	235.761	230.689	66.925
14	959.560	100.483	235.094	7.506
15	1451.362	127.383	558.808	78.973
Average	1142.72502	194.045683	442.690806	41.6685711

Table 5. Integrated cellular and nuclear intensities for radially aligned nanofiber surface.

Image Number	Radial			
	Integrated Cell Intensity Average	Standard Deviation Integrated Cell Intensity	Integrated Nuclei Intensity Average	Standard Deviation Integrated Nuclei Intensity
1	1425.278	299.463	622.449	28.666
2	1253.829	67.525	606.548	45.237
3	1095.705	313.555	583.496	12.367
4	1391.918	118.622	562.123	80.759
5	934.705	5.814	314.953	70.653
6	1385.728	322.370	321.296	68.043
7	1287.619	199.393	631.298	59.736
8	1455.018	294.016	438.800	80.958
9	831.697	202.928	644.547	24.087
10	1063.488	60.330	507.549	77.429
11	971.814	103.550	498.678	44.611
12	980.136	112.718	600.070	56.202
13	834.385	293.726	387.769	10.122
14	1202.385	19.713	397.461	7.399
15	973.360	27.368	671.423	2.822
Average	1139.13771	162.739419	519.230736	44.6060969

Table 6. Cellular, nuclear, and nanofiber orientations for flat control surface.

Control						
Image Number	Cellular Orientation Average	Standard Deviation Cellular Orientation	Nuclear Orientation Average	Standard Deviation Nuclear Orientation	Nanofiber Orientation Average	Standard Deviation Nanofiber Orientation
1	0.022	0.050	-0.320	0.089	N/A	N/A
2	-0.034	0.001	0.717	0.027	N/A	N/A
3	0.055	0.005	0.542	0.038	N/A	N/A
4	0.195	0.037	-0.133	0.040	N/A	N/A
5	-0.004	0.028	0.181	0.038	N/A	N/A
6	0.731	0.085	0.177	0.047	N/A	N/A
7	0.244	0.070	-0.265	0.007	N/A	N/A
8	-0.074	0.041	-0.099	0.044	N/A	N/A
9	0.291	0.029	0.634	0.055	N/A	N/A
10	-0.088	0.042	0.368	0.088	N/A	N/A
11	-0.114	0.082	0.231	0.085	N/A	N/A
12	0.282	0.054	0.164	0.013	N/A	N/A
13	0.541	0.074	-0.400	0.095	N/A	N/A
14	0.011	0.042	0.475	0.063	N/A	N/A
15	0.339	0.025	-0.369	0.003	N/A	N/A
Average	0.1597	0.04437922	0.127	0.0489147	N/A	N/A

Table 7. Cellular, nuclear, and nanofiber orientations for randomly aligned nanofiber surface.

Random						
Image Number	Cellular Orientation Average	Standard Deviation Cellular Orientation	Nuclear Orientation Average	Standard Deviation Nuclear Orientation	Nanofiber Orientation Average	Standard Deviation Nanofiber Orientation
1	0.501	0.079	-0.280	0.007	0.665	0.084
2	0.675	0.090	-0.306	0.047	0.444	0.051
3	-0.303	0.002	0.031	0.008	-0.695	0.057
4	-0.131	0.071	0.099	0.013	0.515	0.053
5	-0.728	0.087	-0.680	0.098	0.220	0.089
6	-0.310	0.008	0.242	0.066	-0.241	0.070
7	0.724	0.091	0.319	0.060	0.352	0.064
8	-0.427	0.099	-0.501	0.005	0.187	0.013
9	0.238	0.056	-0.821	0.057	0.711	0.029
10	-0.492	0.090	-0.004	0.018	0.231	0.044
11	-0.219	0.034	-0.708	0.072	0.763	0.031
12	0.629	0.022	-0.179	0.060	0.149	0.071
13	-0.061	0.080	0.100	0.098	-0.215	0.040
14	0.613	0.096	0.215	0.057	0.229	0.085
15	0.486	0.096	-0.340	0.093	0.287	0.020
Average	0.07961733	0.0667241	-0.188	0.05047819	0.24005429	0.05327857

Table 8. Cellular, nuclear, and nanofiber orientations for radially aligned nanofiber surface.

Image Number	Radial					
	Cellular Orientation Average	Standard Deviation Cellular Orientation	Nuclear Orientation Average	Standard Deviation Nuclear Orientation	Nanofiber Orientation Average	Standard Deviation Nanofiber Orientation
1	0.675	0.083	0.690	0.090	0.693	0.095
2	-0.294	0.042	-0.260	0.051	-0.244	0.048
3	-0.630	0.034	-0.559	0.090	-0.568	0.100
4	-0.141	0.001	-0.043	0.060	-0.098	0.088
5	0.205	0.090	0.259	0.089	0.305	0.052
6	-0.006	0.002	-0.002	0.081	0.062	0.037
7	0.764	0.000	0.770	0.043	0.849	0.038
8	-0.302	0.012	-0.238	0.021	-0.223	0.006
9	0.078	0.097	0.162	0.009	0.078	0.016
10	-0.160	0.089	-0.153	0.014	-0.073	0.083
11	-0.626	0.029	-0.594	0.041	-0.610	0.043
12	-0.153	0.076	-0.058	0.064	-0.121	0.056
13	0.330	0.042	0.373	0.010	0.350	0.012
14	0.708	0.000	0.735	0.081	0.801	0.001
15	0.069	0.058	0.071	0.029	0.075	0.053
Average	0.03444154	0.04364121	0.077	0.05167308	0.08498162	0.04856054

BIBLIOGRAPHY

- 1) Nanci, A. (2007). *Ten Cate's Oral Histology: Development, Structure, and Function*. St. Louis, MO: Mosby.
- 2) Papapanou, P. N., Sanz, M., Buduneli, N., Dietrich, T., Feres, M., Fine, D. H., ... Tonetti, M. S. (2018). Periodontitis: Consensus report of workgroup 2 of the 2017 World Workshop on the Classification of Periodontal and Peri-Implant Diseases and Conditions. *Journal of Periodontology*, 89(Suppl 1), S173–S182.
- 3) Thomson, J. A., Itskovitz-Eldor, J., Shapiro, S. S., Waknitz, M. A., Swiergiel, J. J., Marshall, V. S., & Jones, J. M. (1998). Embryonic stem cell lines derived from human blastocysts. *Science*, 282(5391), 1145–1147.
- 4) Hynes, R. O. (2009). The extracellular matrix: not just pretty fibrils. *Science*, 326(5957), 1216-1219.
- 5) Discher, D. E., Mooney, D. J., & Zandstra, P. W. (2009). Growth factors, matrices, and forces combine and control stem cells. *Science*, 324(5935), 1673-1677.
- 6) Engler, A. J., Sen, S., Sweeney, H. L., & Discher, D. E. (2006). Matrix elasticity directs stem cell lineage specification. *Cell*, 126(4), 677-689.
- 7) McBeath, R., Pirone, D. M., Nelson, C. M., Bhadriraju, K., & Chen, C. S. (2004). Cell shape, cytoskeletal tension, and RhoA regulate stem cell lineage commitment. *Developmental Cell*, 6(4), 483-495.
- 8) Trulsson, M. (2006). Sensory-motor function of human periodontal mechanoreceptors. *Journal of Oral Rehabilitation*, 33(4), 262–273.

- 9) Lynn, B., Tal, M., Waldenlind, E., & Shotton, M. (1979). The origin and distribution of cutaneous, musculocutaneous, and articular branches of the inferior alveolar nerve in the rat. *The Journal of Comparative Neurology*, 184(3), 499–516.
- 10) Kim, Y., & Roh, B. D. (2016). Distribution of the dental occlusal force in normal and periodontitis-affected human subjects: A pilot study using the tensometric system. *Journal of Periodontal & Implant Science*, 46(6), 366–375.
- 11) Gomes, C. A., & Drummond, A. F. (2007). Proprioception: Perception of tooth position in orthodontics. *Dental Press Journal of Orthodontics*, 12(6), 130–156.
- 12) Krishnan, V., & Davidovitch, Z. (2006). Cellular, molecular, and tissue-level reactions to orthodontic force. *American Journal of Orthodontics and Dentofacial Orthopedics*, 129(4), 469.e1–469.e32.
- 13) Roberts-Harry, D., & Sandy, J. R. (2001). Orthodontics. Part 4: Biomechanics and orthodontic tooth movement. *British Dental Journal*, 190(8), 433–437.
- 14) Proffit, W. R., Fields, H. W., Sarver, D. M., & Ackerman, J. L. (2013). *Contemporary Orthodontics*. St. Louis, MO: Mosby.
- 15) Slade, G. D., & Spencer, A. J. (1994). Development and evaluation of the Oral Health Impact Profile. *Community Dentistry and Oral Epidemiology*, 22(6), 398–403.
- 16) Pihlstrom, B. L., Michalowicz, B. S., & Johnson, N. W. (2005). Periodontal diseases. *The Lancet*, 366(9499), 1809–1820.
- 17) Sculean, A., Nikolidakis, D., Nikou, G., & Ivanovic, A. (2016). Chapple, I.L.C., & Stavropoulos, A. Regeneration of periodontal tissues: combinations of barrier membranes and grafting materials—biological foundation and preclinical evidence: A systematic review. *Journal of Clinical Periodontology*, 43(9), S92–S105.

- 18) Haffajee, A. D., & Socransky, S. S. (2002). Dental biofilms: difficult therapeutic targets. *Periodontology 2000*, 28(1), 12–55. [30]
- 19) Slots, J. (2012). Selection of antimicrobial agents in periodontal therapy. *Journal of Periodontal Research*, 47(6), 760–764.
- 20) Cortellini, P., & Tonetti, M. S. (2015). Clinical concepts for regenerative therapy in intrabony defects. *Periodontology 2000*, 68(1), 282–307.
- 21) Esposito, M., Grusovin, M. G., Felice, P., Karatzopoulos, G., Worthington, H. V., Coulthard, P., & Coulthard, P. (2009). Interventions for replacing missing teeth: bone augmentation techniques for dental implant treatment. *The Cochrane Database of Systematic Reviews*, (3), CD003607.
- 22) Mao, J. J., Kim, S. G., Zhou, J., Ye, L., Cho, S., Suzuki, T., ... & Giannobile, W. V. (2017). Regenerative endodontics: barriers and strategies for clinical translation. *Dental Clinics of North America*, 61(4), 839–862.
- 23) Anitua, E. (2014). Platelet-rich plasma: biological background and clinical applications. *Dental clinics of North America*, 58(3), 555–568.
- 24) Clevers, H. (2015). What is an adult stem cell? *Science*, 350(6266), 1319–1320.
- 25) Graf, T., & Enver, T. (2009). Forcing cells to change lineages. *Nature*, 462(7273), 587–594.
- 26) Watt, F. M. (2010). Role of integrins in regulating epidermal adhesion, growth and differentiation. *The EMBO Journal*, 21(15), 3919–3926.
- 27) Dalby, M. J., Gadegaard, N., Tare, R., Andar, A., Riehle, M. O., Herzyk, P., ... & Oreffo, R. O. (2007). The control of human mesenchymal cell differentiation using nanoscale symmetry and disorder. *Nature Materials*, 6(12), 997–1003.

- 28) Yamada, K. M., & Sekiguchi, K. (2015). Molecular basis of laminin–integrin interactions. *Current topics in membranes*, 76, 197-229.
- 29) Frantz, C., Stewart, K. M., & Weaver, V. M. (2010). The extracellular matrix at a glance. *Journal of Cell Science*, 123(24), 4195-4200.
- 30) Murphy, W. L., McDevitt, T. C., & Engler, A. J. (2014). Materials as stem cell regulators. *Nature Materials*, 13(6), 547-557.
- 31) Li, D., & Xia, Y. (2004). Electrospinning of nanofibers: reinventing the wheel? *Advanced Materials*, 16(14), 1151-1170.
- 32) Bognitzki, M., Czado, W., Frese, T., Schaper, A., Hellwig, M., Steinhart, M., ... & Greiner, A. (2001). Nanostructured fibers via electrospinning. *Advanced Materials*, 13(1), 70-72.
- 33) Reneker, D. H., & Chun, I. (1996). Nanometre diameter fibres of polymer, produced by electrospinning. *Nanotechnology*, 7(3), 216.
- 34) Li, M., Mondrinos, M. J., Chen, X., Gandhi, M. R., Ko, F. K., Lelkes, P. I., & Elastogenesis, P. A. (2005). Co-electrospun poly (lactide-co-glycolide), gelatin, and elastin blends for tissue engineering scaffolds. *Journal of Biomedical Materials Research Part A*, 82(3), 992-1003.
- 35) Zhang, Y. Z., Wang, X., Feng, Y., Li, J., & Lim, C. T. (2017). Ramakrishna, S. (2006). *An introduction to electrospinning and nanofibers*. World Scientific.
- 36) Huang, Z. M., Zhang, Y. Z., Kotaki, M., & Ramakrishna, S. (2003). A review on polymer nanofibers by electrospinning and their applications in nanocomposites. *Composites Science and Technology*, 63(15), 2223-2253.

ACADEMIC VITA

Leeann Runkle

EDUCATION: **Bachelor of Science in Biomedical Engineering** Anticipated Graduation:
focus in Digital Imaging and Devices May 2024
Minor in Engineering Leadership Development
The Pennsylvania State University, University Park, PA
Schreyer Honors College
 Clark Scholars Program
 Accepted to Biomedical Engineering One-Year Master's Program at Penn State University
 for admission in fall 2024

TECHNICAL EXPERIENCE:

Undergraduate Research Assistant, Penn State Department of Biomedical Engineering **Jan 2021 – Present**
Regenerative Engineering lab under Dr. Justin Brown

- Cultured Mesenchymal stem cells in different environments to determine the ideal environment for transition into tendon cells.
- Imaged cells using electron microscope and cellular dyeing.
- Altered electrospinning techniques to create radially aligned nanofibers which induced radial cell growth for periodontal ligament synthesis.

Materials Engineering Intern, Corning Incorporated **May – Dec 2022**
Manufacturing, Technology, and Engineering Division

- Designed and ran laboratory experiments focused on high temperature thermal conductivity of materials.
 - Created a new organizational system for internal database of material properties.
 - Networked with and traveled to material suppliers to see how third-party labs conducted property testing.
-

LEADERSHIP EXPERIENCE:

Lead Engineering Peer Advising Leader (EPAL), Penn State Engineering Advising Office **May 2022 – Present**

- Held office hours weekly to aid students in engineering with their schedule, time management, finding tutoring help, and others advising related issues.
- Organized in classroom visits from engineering peer advising leaders to talk about available resources to first year students.

Learning Assistant (LA), Penn State Department of Biomedical Engineering **Aug – Dec 2023**

- Held office hours and study sessions to aid students in the content of BME 406.
- Wrote and graded homework assignments and exams.
- Lectured course content when professor had other obligations.

New Student Orientation Student Aid, Penn State Engineering Advising Office **May – Aug 2023**

- Guided incoming engineering students through the course scheduling process.
 - Spoke to parents and incoming students about personal experience transitioning to college and the various resources available to aid in the transition.
-

INVOLVEMENT: Leadership Board, Clarks Scholars Program 2020-2024
 Member, Society of Women Engineers (National & PSU) 2020-2024
 Member, Biomedical Engineering Society (National & PSU) 2021-2024
 Member, Engineering Leadership Society 2021-2024

HONORS: Recipient, Clark Scholarship (2020-2024)
 Recipient, Druanne Schreyer Renaissance Scholarship (2020-2024)